Int. J. Heat Mass Transfer. Vol. 36, No. 12, pp. 3077–3088, 1993
Printed in Great Britain

0017–9310/93 $6.00 + 0.00

Heat and humidity transfer in non saturated porous media: capillary hysteresis effects under cyclic thermal conditions

C. H. A. MOLENDA, P. CRAUSSE and D. LEMARCHAND
Institut de Mécanique des Fluides, Avenue du Prof. Camille Soula, 31400 Toulouse Cedex, France

(*Received* 10 *February* 1992 *and in final form* 10 *December* 1992)

Abstract—An analysis of the influence of capillary hysteresis in the humidity migration in porous media is presented. Several situations have been considered: experimental and numerical study of transfer phenomena in porous media at impermeable boundaries, numerical simulation of the thermo-hydraulic behaviour of the cellular concrete wall under cyclic thermal conditions. Effects of temperature on capillary properties and the relaxation time of the liquid flux by capillary effects, are also taken into account and studied.

1. INTRODUCTION

HUMID porous media can be submitted to temperature variations whether during natural physical situations (night and day cycles at ground and building surface) or industrial situations (drying farm-produce or building materials). Some internal displacements of moisture take place, the direction of which will be linked to the temperature gradients. Indeed, porous media may be alternately in position of draining (moisture loss) or of wetting (moisture gain), during for instance, cyclic variations of surface hygro-thermic conditions.

The observations of many researchers have shown that the retention and transport properties of moisture of these media can be different in draining or wetting, thus dependent on the porous medium hydraulic history. This fact is particularly pronounced when the liquid phase of the humid porous medium is continuous. The moisture retention properties, defined by the capillary suction potential ψ, temperature T and the mean local water content ω_l manifests a pronounced hysteretic character. To guarantee a rigorous approach when estimating the coupled phenomena of heat and mass transport in porous media, the influence of hydraulic history on the transport properties should be taken into account. In that way simulations are needed to determine the importance of the hysteresis on the phenomena predictions.

Recently, the authors have presented a bibliographic synthesis [1], concerning the influence of capillary hysteresis on the coupled transfers of moisture and heat in non-saturated porous media under time-invariant boundary conditions. The results obtained showed that if hysteresis is not considered in the case of a closed system subjected to a weak temperature gradient with mean water content situated in the middle of the hysteresis cycle, it can lead to important errors concerning the estimations of moisture distributions. On the other hand, the heat transfer due to a low variation of thermal conductivity with the water content ω_l, is not affected to any great extent by hysteresis capillary.

The purpose of this paper, which is an extension of our previous work, is to clarify some questions relative to the effects of capillary hysteresis in the estimation of heat and mass transfer phenomena when:

- the average humidification of the medium is situated at the boundary of the hysteresis cycle (low water content domain),
- the thermal boundary conditions are cyclic, representative for instance of a night and day cycle,
- the influence of one relaxation time of the moisture flux in liquid phase is taken into account in the simulations.

2. MATHEMATICAL MODEL

The modelisation of mass and energy transfer in non saturated porous media is made considering a continuum equivalent to the porous medium. The transport equations variables are relative to macroscopic properties of a porous medium block, considered as the Representative Elementary Volume, REV [2].

The basic assumptions considered are:

- the solid phase which constitutes the porous medium is rigid and isotropic in a macroscopic sense,
- the gaseous phase total pressure is uniform and constant,
- there is a local thermodynamic equilibrium between the phases within porous medium,
- there are no chemical reactions between the solid, liquid and gaseous phase,
- heat transfer by radiation is negligible,
- dissipation effects in the flow are negligible,
- the heat of wetting is neglected.

NOMENCLATURE

a	volumetric gas content
a_k	volumetric gas content below which liquid continuity begins
B_T	coefficient of thermal volume expansion of water
C_i	specific heat of phase i
C^*	specific heat of porous medium
D	diffusion coefficient of water vapor in air
D_{Tv}	transport coefficient for vapor flux due to thermal gradient
$D_{\psi v}$	transport coefficient for vapor flux due to ψ gradient
g	gravitational acceleration
h	enthalpy
J_{lc}	capillary–liquid flux
J_{lg}	gravity–liquid flux
J_q	conduction heat flux
J_v	vapor flux
K	hydraulic conductivity
$\mathbf{k}$	unit vector in the positive z direction
L	latent heat of evaporation
M	molar mass of water
P	pressure
P_h	hydrostatic pressure
R	universal gas constant
t	time
T	temperature
V	volumetric trapped air content.

Greek symbols

α	tortuosity
ε	porosity
θ_l	volumetric liquid content
λ	thermal conductivity
λ_a	air thermal conductivity
λ_{ve}	effective vapor thermal conductivity
ρ	density
ρ_0	nominal density of the porous medium
τ	relaxation time
ϕ	relative humidity
ψ	moisture potential or suction
ω_l	liquid content $\cong$ moisture content
ω_v	vapor content.

Subscripts

0	initial value or nominal value
a	air
l	liquid
v	vapor
s	solid
q	heat
vs	vapor saturation.

The mathematical model used is already presented in ref. [1]. Therefore, the equations are given here in their final form.

Equation (1) represents the mass conservation, equation (2) represents the energy conservation and equation (3) the relation between the variables ψ–ω_l–T which depend on the porous medium thermo-hydraulic history.

$$(1-A)\frac{\partial\omega_l}{\partial t}+B\frac{\partial\psi}{\partial t}+C\frac{\partial T}{\partial t}=-\frac{1}{\rho_0}\nabla\cdot(J_{lc}+J_{lg}+J_v) \tag{1}$$

$$(h_l-Ah_v)\frac{\partial\omega_l}{\partial t}+Bh_v\frac{\partial\psi}{\partial t}+(C^*+h_vC)\frac{\partial T}{\partial t}=-\frac{1}{\rho_0}\nabla\cdot[J_q+h_l(J_{lc}+J_{lg})+h_vJ_v] \tag{2}$$

$$\omega_l=\omega_l[\psi(t'),t'\leqslant t,T] \tag{3}$$

$$\tau\frac{\partial J_{lc}}{\partial t}+J_{lc}=-\rho_lK\nabla\psi \tag{4}$$

$$J_{lg}=-\rho_lK\mathbf{k} \tag{5}$$

$$J_v=-D_{\psi v}\nabla\psi-D_{Tv}\nabla T \tag{6}$$

$$J_q=-\lambda\nabla T \tag{7}$$

$$D_{\psi v}=\alpha aD\frac{P}{P-P_v}\left(\frac{M}{RT}\right)^2P_{vs}g\phi \tag{8}$$

$$D_{Tv}=(a+\theta_lg(a))\eta\Gamma D\frac{P}{P-P_v}\frac{M}{RT}\phi P_{vs}\times\left(\frac{1}{P_{vs}}\frac{dP_{vs}}{dT}-\frac{\psi Mg}{RT^2}\right) \tag{9}$$

$$C^*=C_s+\omega_lC_l+\omega_vC_v \tag{10}$$

$C_i(i=\text{s, l, v})$ is the specific heat of the ith phases.

2.1. ψ–ω_l–T relationship modelisation

In the modelisation of ψ–ω_l relationship, Mualem's model II [3] and Mualem and Dagan's model III [4] will be used. The thermal effects will be considered through a model for the $(\partial\psi/\partial T)_{\omega_l}$ parameter.

For the simulation inside hysteresis cycle, Mualem's model II requires only, as experimental data, boundary curves of the cycle (mains draining and imbitition curves). During a wetting, after a series of wetting and draining cycles, the value of Ω defined as the difference between the water content and the residual water content, $\Omega=\omega_l-\omega_{lmin}$, is given by:

$$\Omega\begin{pmatrix}\psi_1 & \cdots & \psi\\ \psi_{\min} & \psi_2 & \cdots & \psi_N\end{pmatrix} = \Omega_w(\psi) + [\Omega_w(\psi_{N-1}) - \Omega(\psi)]H(\psi_N) + \sum_{j=1}^{(N/2)-1} [\Omega_w(\psi_{2j-1}) - \Omega_w(\psi_{2j+1})]H(\psi_{2j}). \quad (11)$$

The left side of this equation shows that the process consists firstly of an increase from $\psi_{\min}$ to ψ_1 (wetting), then a decrease from ψ_1 to ψ_2 (draining), again an increase from ψ_2 to ψ_3 and so on... Ω_w is the value of $\Omega(\psi)$ read on the main wetting curve.

The value of Ω during a draining is given by the relation:

$$\Omega\begin{pmatrix}\psi_1 & \cdots & \psi_N\\ \psi_{\min} & \psi_2 & \cdots & \psi\end{pmatrix} = \Omega_w(\psi) + [\Omega_w(\psi_N) - \Omega_w(\psi)]H(\psi) + \sum_{j=1}^{(N-1)/2} [\Omega_w(\psi_{2j-1}) - \Omega_w(\psi_{2j+1})]H(\psi_{2j}). \quad (12)$$

The function $H(\psi)$ is defined by:

$$H(\psi) = \frac{\Omega_d(\psi) - \Omega_w(\psi)}{\Omega_u - \Omega_w(\psi)} \quad (13)$$

$\Omega_d(\psi)$ is the value of $\Omega(\psi)$ read on the main draining curve and Ω_u is the maximum water content.

When a large part of the hysteresis field is situated in the range of air-entry-values, significant differences between experiments and estimations of Mualem's model II have been observed [4]. This fact leads Mualem and Dagan to introduce model III. This model based on Mualem's model II, uses additional functions to consider pore blocking by water, with high water content, and by air when the water content is low. These two functions are considered as depending only on the water content and not on the hydraulic history. As Mualem and Dagan commented, the correction function for the pore blocking by air seems to be of minor importance. For that reason only the correction function for the pore blocking by water (F_c) will be considered in this work. According to this model, the value of Ω during a wetting is given by:

$$\Omega\begin{pmatrix}\psi_1 & \cdots & \psi\\ \psi_{\min} & \psi_2 & \cdots & \psi_N\end{pmatrix} = \Omega(\psi_N) - F_c(\Omega_N)[1 - G(\psi_N)][\Omega_w(\psi) - \Omega_w(\psi_N)]. \quad (14)$$

During a draining this value is given by:

$$\Omega\begin{pmatrix}\psi_1 & \cdots & \psi_N\\ \psi_{\min} & \psi_2 & \cdots & \psi\end{pmatrix} = \Omega(\psi_N) - F_c(\Omega)[1 - G(\psi)][\Omega_w(\psi_N) - \Omega_w(\psi)]. \quad (15)$$

The functions $F_c(\Omega)$ and $G(\psi)$ are determined by the help of the main hysteresis cycle and a primary draining curve. The application of equation (15) for the main draining curve gives:

$$\Omega_u - \Omega_d(\psi) = F_c(\Omega)[1 - G(\psi)][\Omega_u - \Omega_w(\psi)] \quad (16)$$

and in the case of a primary draining curve:

$$\Omega_w(\psi_1) - \Omega(\psi) = F_c(\Omega)[1 - G(\psi)][\Omega_w(\psi_1) - \Omega_w(\psi)]. \quad (17)$$

The equations (16) and (17) make it possible to determine simultaneously $F_c(\Omega)$ and $G(\psi)$.

As in ref. [1], the parameter $(\partial\psi/\partial T)_{\omega_l}$ is modelised by equation (18) in which different values of N will be considered during the simulations:

$$\left(\frac{\partial\psi}{\partial T}\right)_{\omega_l} = N\gamma\psi \quad (18)$$

$\gamma = (1/\sigma)(d\sigma/dT)$ is the superficial tension coefficient.

3. NUMERICAL FORMULATION

The method used to solve the equation set in bi-dimensional fields is the classical finite volume method, fully implicit [5]. Considering the capillary liquid flux, the existence of a relaxation time requires a modification of the discretization in time. The solution of equation (4), is:

$$J_{lc} = J_{lc0}\exp\left(\frac{-t}{\tau}\right) - \rho_l K\nabla\psi\left[1 - \exp\left(\frac{-t}{\tau}\right)\right] \quad (19)$$

in which J_{lc0} is the initial flux. In a time interval Δt the flux is determined by:

$$\int_{\Delta t} J_{lc}\,dt = J_{lc}^n\tau\left[1 - \exp\left(\frac{-\Delta t}{\tau}\right)\right] - \rho_l K\nabla\psi^{n+1}\left\{\Delta t - \tau\left[1 - \exp\left(\frac{-\Delta t}{\tau}\right)\right]\right\}. \quad (20)$$

The superscript n indicates values at the initial instant of a time interval and $n+1$ at its end. The discretization shown in equation (20) is also valid for the other flux, considering a relaxation time zero [6].

To solve equation (3), having a model defining the variation of suction with temperature at a constant water content, it is easier to explain the variable ψ instead of ω_l. The suction ψ is a function of its value at the obtention temperature of the experimental hysteresis cycle, ${}^0\psi$ (which only depends on water content and hydraulic history) and of temperature:

$$\psi = f({}^0\psi, T). \quad (21)$$

The analysis of equation (21) shows that:

$$\psi = {}^0\psi\left(\frac{\sigma(T)}{{}^0\sigma}\right)^N \quad (22)$$

where ${}^0\sigma$ is the water superficial tension at the temperature of the experimental hysteresis cycle. The water content evolution in each control volume is given by:

$$\frac{d\omega_l}{dt} = \left(\frac{d\omega_l}{d\psi}\right)_T \frac{d\psi}{dt} - \left(\frac{\partial\omega_l}{\partial\psi}\right)_T \left(\frac{\partial\psi}{\partial T}\right)_{\omega_l} \frac{dT}{dt} \quad (23)$$

and using equation (22):

$$\frac{d\omega_l}{dt} = \left(\frac{\partial\omega_l}{\partial^0\psi}\right)_T \left(\frac{^0\sigma}{\sigma}\right)^N \frac{d\psi}{dt} - \left(\frac{\partial\omega_l}{\partial^0\psi}\right)_T {}^0\psi N\gamma \frac{dT}{dt}. \quad (24)$$

The discretization of this equation leads to:

$$\omega_l^{n+1} - \omega_l^n = \left(\frac{\partial\omega_l}{\partial^0\psi}\right)^{n+1} \left(\frac{^0\sigma}{\sigma(T^{n+1})}\right)^N [\psi^{n+1} - \psi^n] - \left(\frac{\partial\omega_l}{\partial^0\psi}\right)^{n+1} {}^0\psi(\omega_l^{n+1}) N\gamma(T^{n+1})[T^{n+1} - T^n]. \quad (25)$$

The values of $(\partial\omega_l/\partial^0\psi)$ are given by Mualem's model II or Mualem and Dagan's model III. Considering model II:

—during draining:

$$\left(\frac{\partial\omega_l}{\partial^0\psi}\right) = [1 - H(^0\psi)]\left(\frac{\partial\omega_l}{\partial^0\psi}\right)_{imb} + [\omega_l(^0\psi_N) - \omega_l(^0\psi)]_{imb} \frac{\partial H}{\partial^0\psi} \quad (26)$$

—during wetting:

$$\left(\frac{\partial\omega_l}{\partial^0\psi}\right) = [1 - H(^0\psi_N)]\left(\frac{\partial\omega_l}{\partial^0\psi}\right)_{imb}. \quad (27)$$

In the two previous equations, subscripts imb and N mean respectively, the values taken from the main wetting curve, and the values of the last turn back point draining/wetting or wetting/draining.

The case of Mualem and Dagan's model III gives:

—during draining:

$$\left(\frac{\partial\omega_l}{\partial^0\psi}\right) = F_c(\omega_l)\left\{[\omega_l(^0\psi_N) - \omega_l(^0\psi)]_{imb} \frac{\partial G}{\partial^0\psi} + [1 - G(^0\psi)]\left(\frac{\partial\omega_l}{\partial^0\psi}\right)_{imb}\right\} \quad (28)$$

—during wetting:

$$\left(\frac{\partial\omega_l}{\partial^0\psi}\right) = F_c(\omega_{lN})[1 - G(^0\psi_N)]\left(\frac{\partial\omega_l}{\partial^0\psi}\right)_{imb}. \quad (29)$$

The solution of the equation set is realized in an interactive way by using line by line solution method [5]. First the energy conservation equation is considered, then the mass equation and finally the equation (25) for the determination of the water content. Time steps are variable, according to the problem analysed, and determined by preliminary tests.

4. APPLICATIONS

Within the context of this work, the following have been realised:

- a comparison between experimental data and numerical simulations concerning a thermomigration process in a closed system with low water content, close to the water content limit of the hysteresis cycle, with constant boundary conditions,
- a numerical study of the hysteresis influence on system under thermal conditions which are time-variable. To this purpose, two physical configurations studied in ref. [1] have been considered: a closed and an open system,
- a brief study of the influence of the relaxation time of the liquid flux by capillarity.

The hysteresis of absorption isotherms is not considered here. The analysis of its influence will be realised in a further work.

4.1. *Closed system*

The set-up and the experimental procedures used are described in refs. [1, 6]. The closed system strictly speaking is a cylindrical cell 35 cm long, 6 cm in diameter filled with damp sand. The quartz sand used here is the same one used for the previous work [1]. This material was chosen by Nguyen-Tan [7] who determined the hydraulic conductivity, function of water content, the main wetting and draining curves, and several primary curves. Figure 1 shows the hysteresis cycle and the primary draining curve used to obtain $H(\psi)$ function of Mualem's model II and $F_c(\omega_l)$ and $G(\psi)$ functions of Mualem and Dagan's model III.

The mean water content of the sandy medium considered is of 0.03 kg kg^{-1}. During the first experiment three cells underwent a low thermal gradient (54°C to the hot side and 20°C to the cold side) 12 days later, the determination of moisture distribution was obtained by a destruction method (slicing the porous

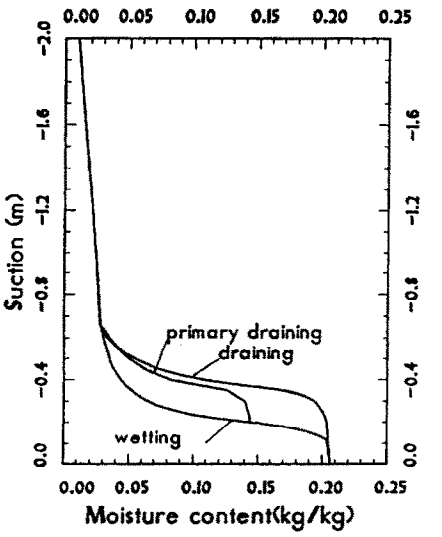

FIG. 1. Hysteresis cycle (quartzic sand).

medium and over drying the samples [6]). A series of numerical simulations has been realised with and without hysteresis and with different values of N (equation (18)). These simulations have been developped according to two types of procedure:

- if only the main wetting curve or the complete hysteresis cycle are taken into account, the initial conditions of water content and capillary suction are chosen on the main wetting curve,
- if the main draining curve is considered, the initial conditions correspond to a point on this curve. The initial temperature is 20°C, and the flux relaxation period during a liquid phase is nil. When the complete hysteresis cycle is taken into account, Mualem and Dagan's model III [4] is used.

The simulations have been realised in a rectangular domain 350 × 60 mm, divided into 210 finite volumes and the comparison between the experimental results was done thanks to vertical averages. The results are presented in Fig. 2 in which the left side corresponds to the hot side of the cell.

In a second experiment a cell underwent a thermal gradient for 12 days and was then put into isotherm at 20°. Figure 3 shows the moisture distribution after 35 days in isothermal conditions. Figures 4 and 5 present comparative results of the numerical simulation for 28 and 68 days in isothermal conditions after 12 days of thermal gradient.

4.1.1. *Thermal cyclic boundary conditions.* To check situations where hysteresis has been taken into account and where thermal conditions are cyclic on one side of the closed system, the following boundary conditions have been used for the temperature:

$$T(0, t) = (20 + 15 \sin(wt))°C \quad (30)$$

$$T(L, t) = 20°C. \quad (31)$$

According to condition (30), temperature can vary from 5 to 35°C during a $2\pi/w$ period. In this work, only the results concerning a 48 h period are presented. In ref. [6], the interested readers will find the results concerning other periods. The considered value of N is 3.

Two mean water contents in the closed system have been considered: 0.11 kg kg^{-1}, in the middle of the hysteresis cycle (Fig. 6) and 0.03 kg kg^{-1}, close to the boundary water content of the hysteresis cycle (Fig. 7).

4.1.2. *Analysis of the results.* The comparison between the experimental results and the numerical simulations shows, firstly a satisfactory concordance taking into consideration the experimental difficulties of precisely determining the transport coefficients and the capillary properties of the porous medium. Besides, taking the hysteresis into account did not significantly modify the moisture distributions given by the simulations. This result completes the results obtained in ref. [1] for high water content, where taking hysteresis effects into account noticeably improved the agreement with the experimental results. As the thermal distribution in the closed system strongly depends on the moisture distribution, these conclusions can be widened to the capillary hysteresis influence on to the heat transfers.

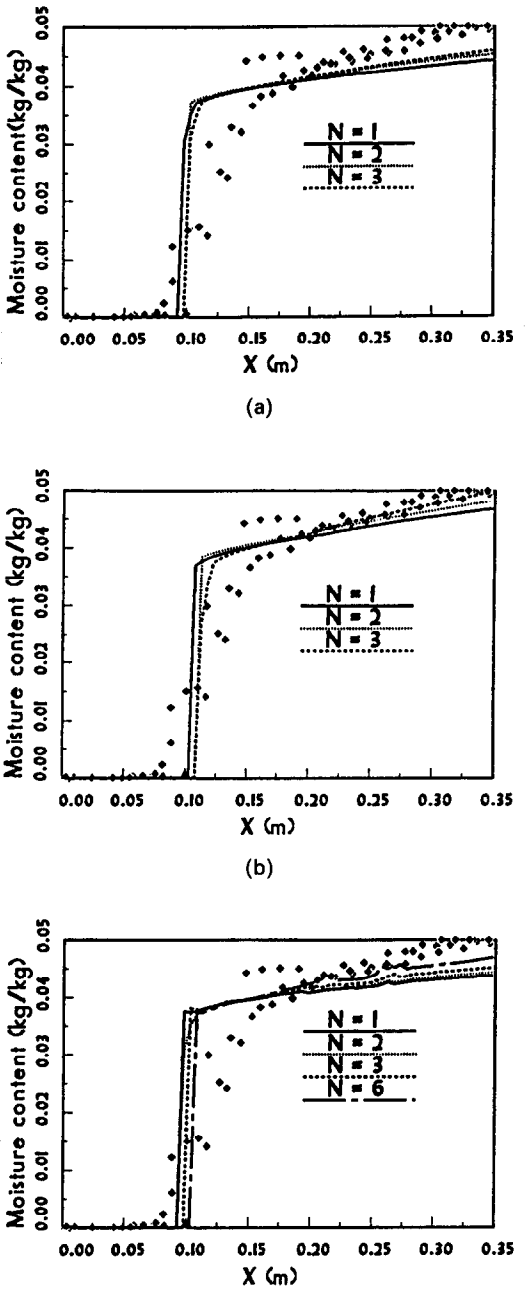

FIG. 2. Comparison between experimental and numerical results—12 days with temperature gradient. (a) Simulation with hysteresis, model III; (b) Wetting curve; (c) Draining curve.

Simulations with different values of N showed the sensitivity of moisture distributions to variations of $(\partial\psi/\partial T)_{\omega_l}$ parameter values. Increasing this parameter also increases the length of the dry zone and causes

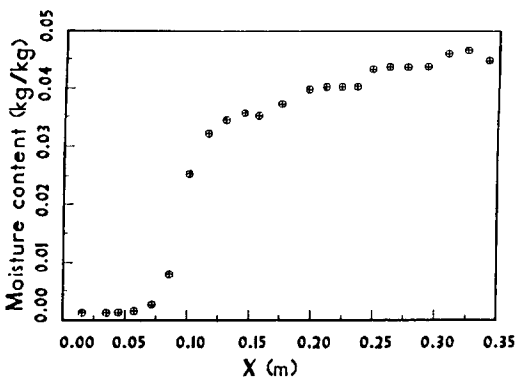

FIG. 3. Experimental result—12 days with thermal gradient and 35 days in isothermal conditions (20°C).

a greater slope of the moisture profile in the moistened zone.

The simulation results with cyclic thermal conditions on one face of the closed system show that when the water content is low, the hysteresis influence can be neglected but when water content is high, then this influence can become important. Besides, when the water content is low, simulations with a variable temperature between 35 and 5°C for a 48 h period showed that in spite of the formation of a narrow dry zone, there is vapor condensation in the wall where the temperature varies.

4.2. *Open system*

The problem of a cellular concrete wall under boundary conditions of temperature and relative humidity, invariant in time, has already been analysed [1]. This study realised numerical simulations with a time variable temperature on one side of the wall. The simulations were done in a 200 mm long unidimensional area divided into 40 finite volumes. The hysteresis model used is Mualem's simplified model II [8]. The necessary experimental data were obtained in refs. [6, 9, 10]. As an example, the value of N is 3 and the relaxation time of the capillary liquid flux is considered to be nil. The initial conditions chosen for simulations are:

—water content: 0.02 kg kg^{-1}
—temperature: 20°C
—capillary suction: like that described for the closed system.

The boundary conditions considered are:

$$T(0,t) = 20°C \tag{32}$$

$$\phi(0,t) = 50\% \tag{33}$$

$$T(L,t) = (20+15\sin(wt))°C \tag{34}$$

$$\phi(L,t) = 90\%. \tag{35}$$

Figure 8 shows the results obtained by considering a thermal variation cycle equal to 24 h.

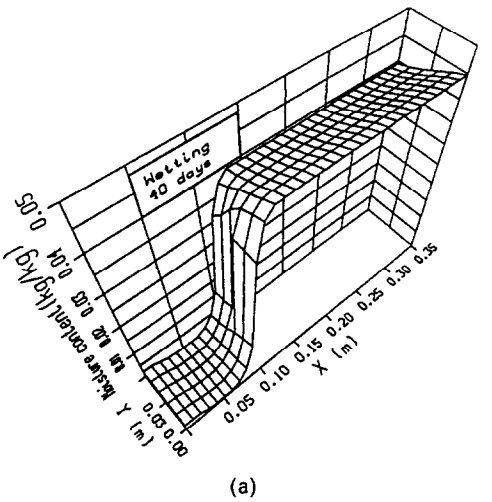

(a)

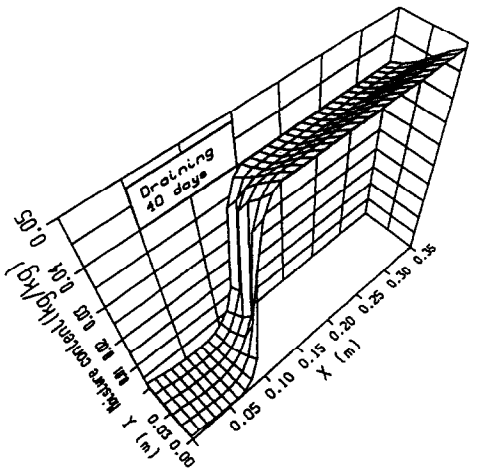

(b)

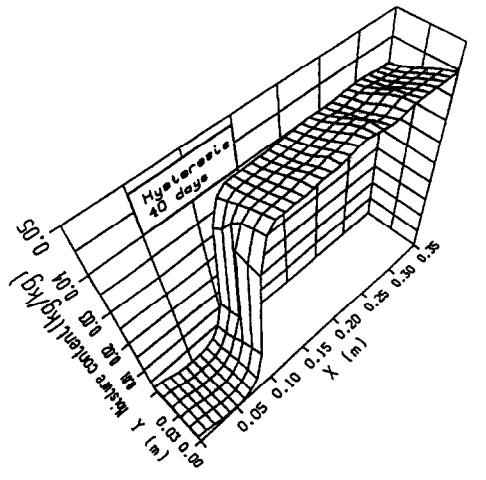

(c)

FIG. 4. Numerical simulations—12 days with thermal gradient and 28 days in isothermal conditions (20°C). (a) Wetting curve; (b) draining curve; (c) hysteresis cycle.

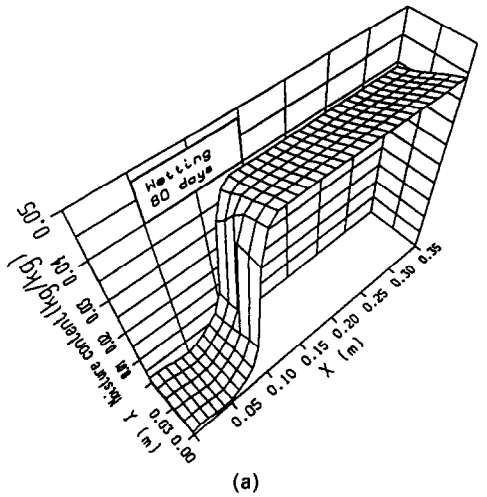

(a)

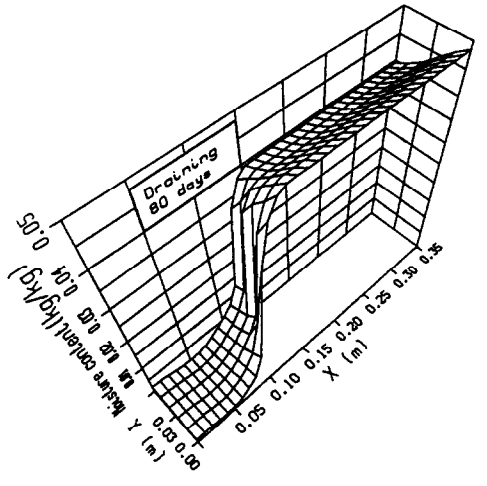

(b)

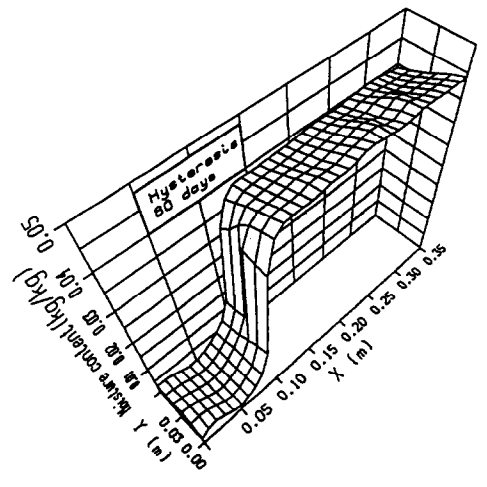

(c)

FIG. 5. Numerical simulations—12 days with thermal gradient and 68 days in isothermal conditions (20°C). (a) Wetting curve; (b) draining curve; (c) hysteresis cycle.

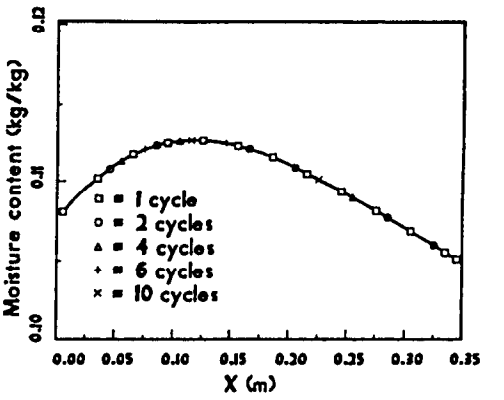

(a)

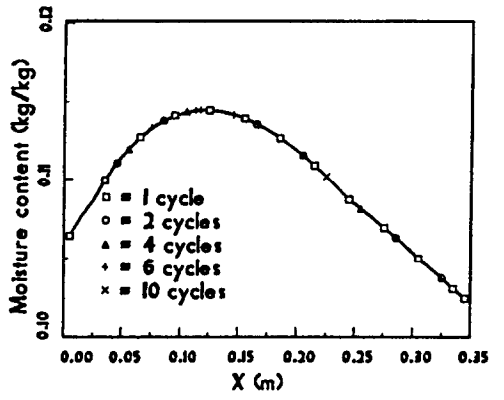

(b)

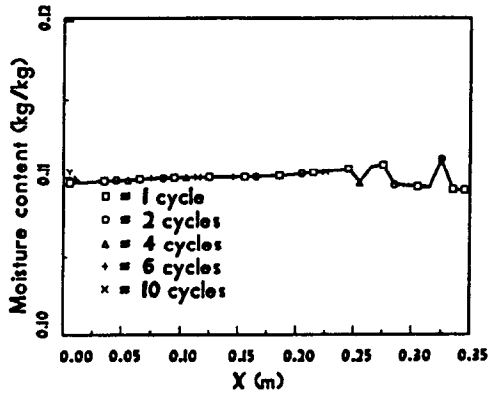

(c)

FIG. 6. Cyclic thermal conditions—Quartzic sand. Numerical simulations. (a) Wetting curve; (b) draining curve; (c) hysteresis cycle.

4.2.1. *Analysis of the results.* Taking hysteresis into account shows intermediary moisture distributions between the ones given by the simulations using only the main wetting curve and the main draining curve. In an analysis using other periods for thermal cyclic variation, Molenda [6] found that the simulation

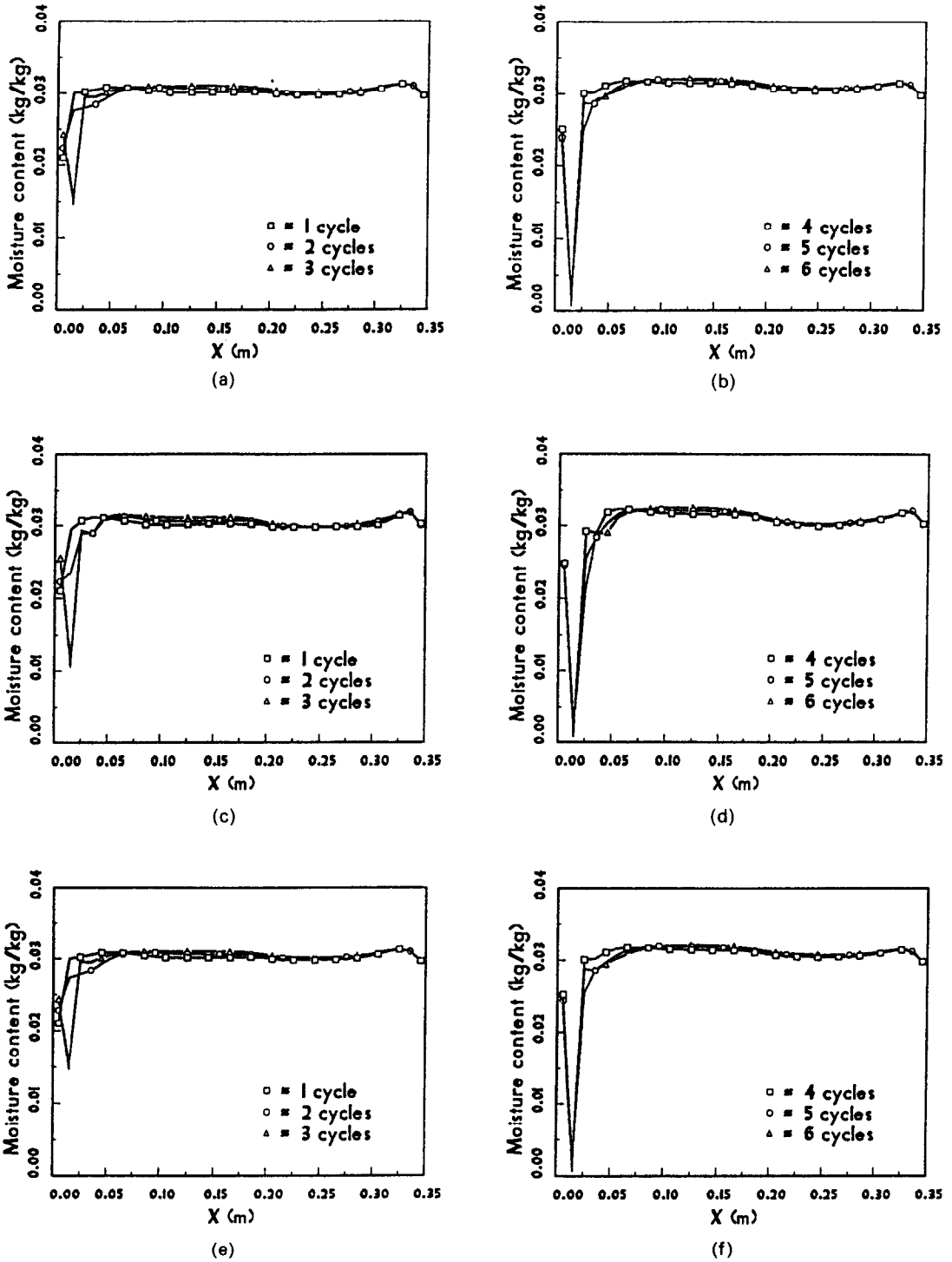

FIG. 7. Cyclic thermal conditions—Quartzic sand. Numerical simulations. (a), (b) Wetting curve; (c), (d) draining curve; (e), (f) hysteresis cycle.

results with hysteresis are generally closer to the simulation results made with the main wetting curve only. This is due to the fact that during the simulations which take the whole hysteresis cycle into account, the initial conditions of porous medium were considered on the main wetting curve.

These results show that when boundary conditions depend on time (cyclic in the present case), it may be necessary to take capillary hysteresis into account so as to determine moisture distributions. Indeed, in such particular physical situations, the porous medium surface undergoes drying and humidification conditions

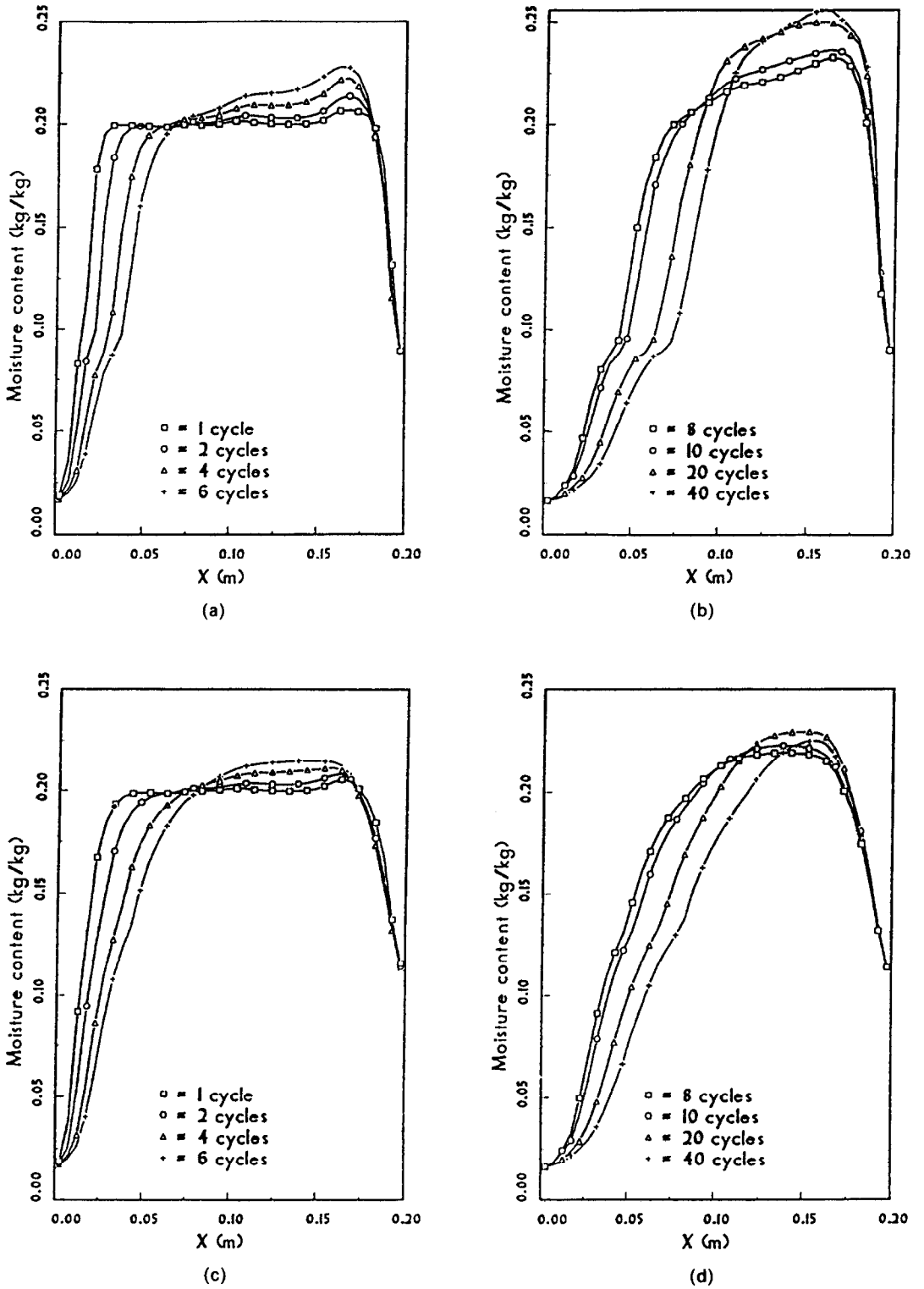

FIG. 8. Cyclic thermal conditions—Cellular concrete. Numerical simulations. (a), (b) Wetting curve; (c), (d) draining curve; (e), (f) hysteresis cycle.

linked to the thermal variations. To establish precisely how the material will react to such promptings, the whole capillary hysteresis cycle must be considered. On the other hand, when the thermal boundary conditions do not change with time, this rigourous approach becomes unnecessary.

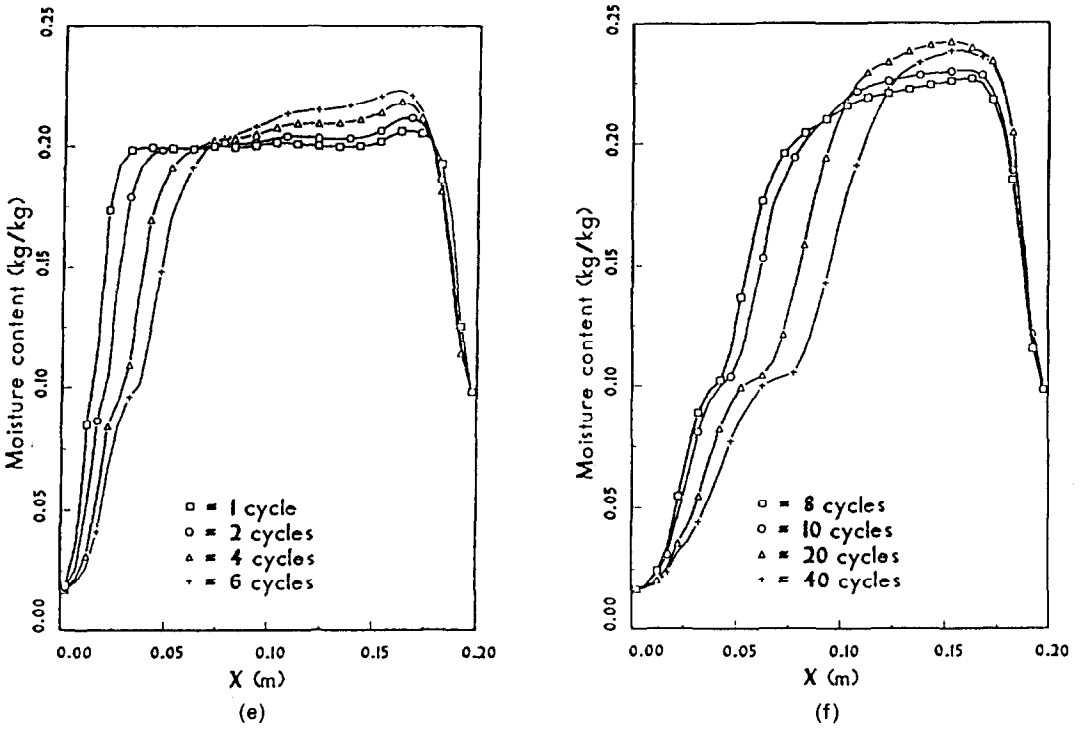

FIG. 8.—*Continued.*

4.3. *Influence of the relaxation time of capillary liquid flux*

The analysis of the influence of the relaxation time lay down two problems:

- ignoring the value of τ: to our knowledge, there is no other work relating to the time relaxation of capillary liquid flux than that of Luikov [11]. The relaxation time of heat flux in a non-homogeneous medium is also unknown. Kaminski's experimental results situate them between 10 and 50 s [12]. But other authors quoted by Kaminski suggest values between 10 and several thousands of seconds,
- use of appropriate numerical methods: time steps must be lower or approximately equal to the relaxation time. This can be too penalising if τ is lower than 1 s.

The numerical method used for this work is fully implicit. This method is robust but sometimes requires too many interactions for the equations are not linear, particularly when the phase change terms prevail. Normally, this prevents simulations of long transitory systems with too short a time step.

In the present work, relaxation times between 1 and 100 s have been considered and their influence on two physical situations are analysed:

- a closed system (sandy medium) with homo-

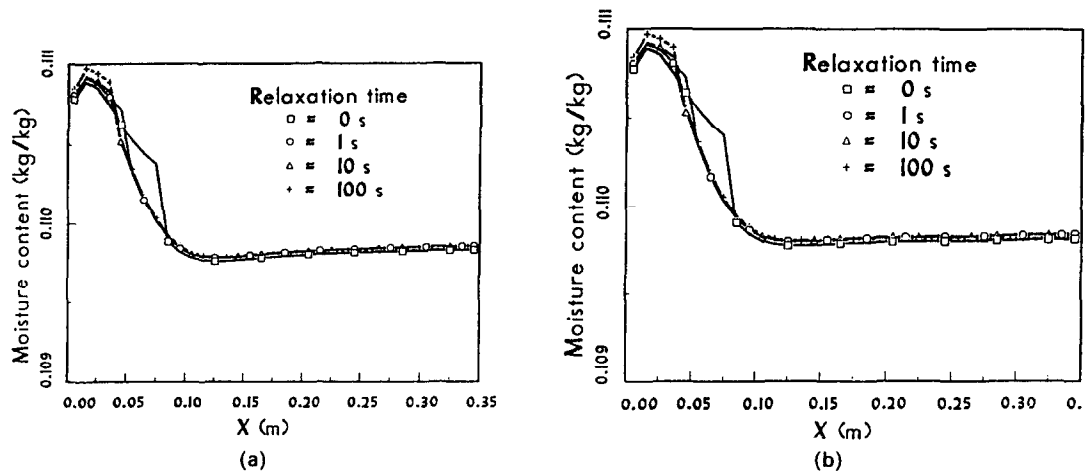

FIG. 9. Influence of the relaxation time—Quartzic sand. (a) After 2 cycles; (b) after 6 cycles.

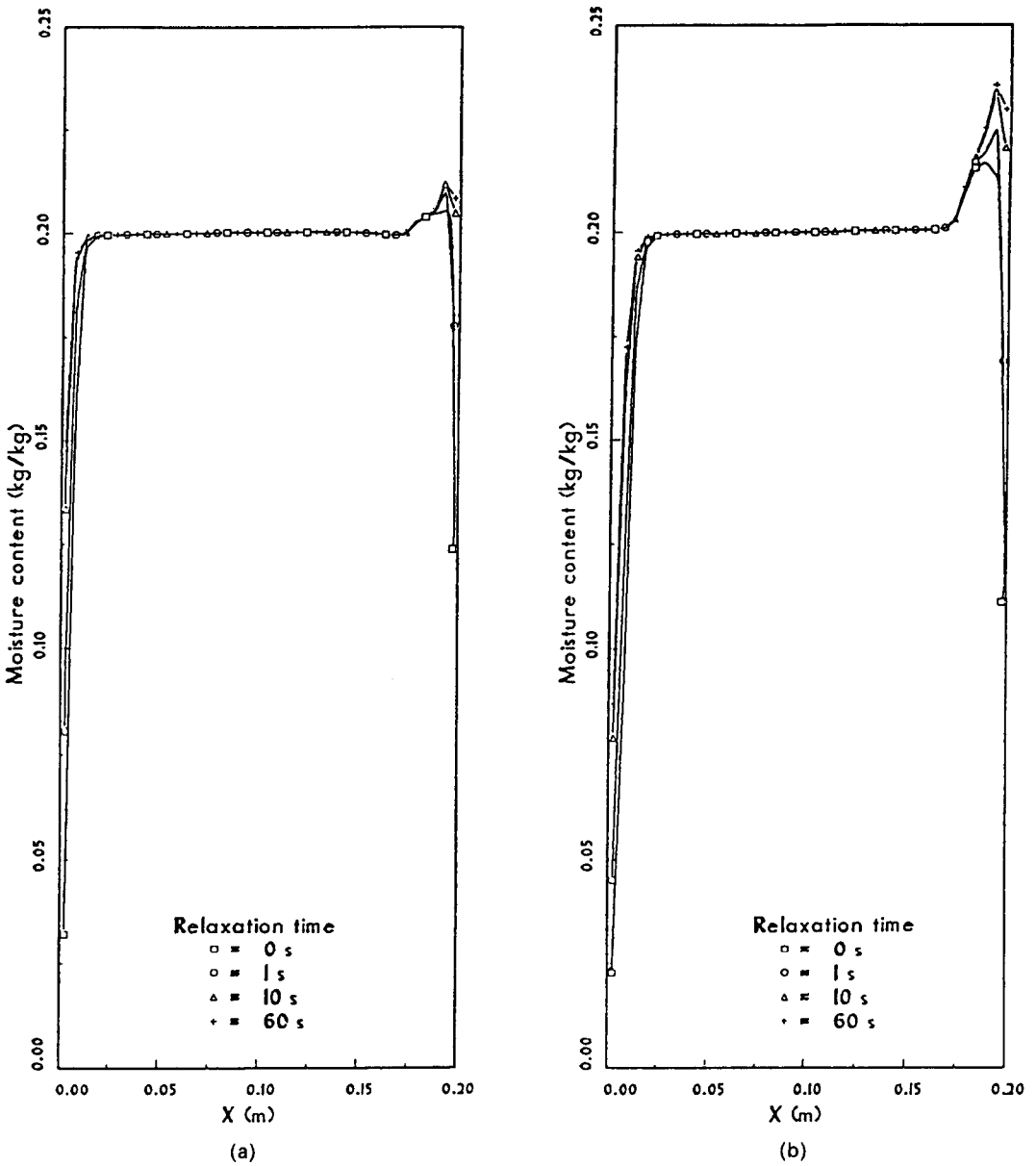

FIG. 10. Influence of the relaxation time—Cellular concrete. (a) After 2 cycles; (b) after 6 cycles.

geneous initial water content $\omega_1 = 0.11\ \text{kg kg}^{-1}$, initial suction $\psi = -0.31$ m, initial temperature 20°C. The thermal boundary conditions are given by equations (30) and (31). Period equal to one hour,

- an open system (cellular concrete), initial water content $\omega_1 = 0.20$ kg kg^{-1}, initial suction $\psi = -108.20$ m. Initial conditions are given by equations (32) and (35). Period equal to one hour.

For both configurations, simulations were made taking hysteresis into account. Mualem and Dagan's model III was used for the closed system and the simplified model II for the open system. The time step chosen for every simulation was 1 s. The initial capillary liquid flux is nil.

The results obtained (relative to the closed system in Fig. 9, and to the open system in Fig. 10) show that in the closed system, the influence of relaxation times below 100 s can be neglected, but the same conclusion cannot be applied to the open system. As the number of the cycles and/or the relaxation time increases, the accumulation of liquid in the cellular concrete wall, near the right boundary, also increases. This is due to the decrease in the capillary liquid flux because of the relaxation time.

5. CONCLUSION

The analysis done throughout this article, which completes the analysis realised in ref. [1], shows that

the importance of taking capillary hysteresis into account to establish the moisture and heat coupled transfer in non saturated porous medium is problem-dependent. This can become important, for instance, in thermomigration problems in closed systems, with higher water content, or in open systems with boundary conditions depending on time. On the other hand, in a closed system with low water content and in an open system with constant boundary conditions, the influence of hysteresis does not seem to be so important.

Besides the capillary hysteresis effects, the influences of the relaxation time of the capillary liquid flux and the parameter value $(\partial\psi/\partial T)_{\omega_1}$ were analysed.

The simulations show that the influence of relaxation time longer than one second could be important in open systems with cyclic boundary conditions. In such cases, the relaxation time helps moisture accumulation in condensation zones, because it slows down the variations of the capillary liquid flux.

The study of the numerical results sensitivity to the variations of $(\partial\psi/\partial T)_{\omega_1}$, in closed systems with low water content showed less sensitivity than in the case of high water contents. Besides the influence on the slope of the distribution of water contents in the damp zone, the results obtained brought to the fore the effects of this parameter on the development of the dry zone. On the other hand, choosing several values of N during simulations does not change the conclusions of this work, concerning the influence of capillary hysteresis on the establishment of mass and heat transfer phenomena in porous media [6].

REFERENCES

1. C. H. A. Molenda, P. Crausse and D. Lemarchand, The influence of capillary hysteresis effects on the humidity and heat coupled transfer in non-saturated porous medium, *Int. J. Heat Mass Transfer* **35,** 1385–1396 (1992).
2. Y. Bachmat and J. Bear, Macroscopic modelling of transport phenomena in porous media. 1—The continuum approach, *Transport in Porous Media* **1,** 213–240 (1986).
3. Y. Mualem, A conceptual model of hysteresis, *Water Resour. Res.* **10,** 514–520 (1974).
4. Y. Mualem and G. Dagan, A dependent domain model of capillary hysteresis, *Water Resour. Res.* **11,** 452–460 (1975).
5. S. V. Patankar, *Numerical Heat Transfer and Fluid Flow.* Hemisphere, New York (1980).
6. C. H. A. Molenda, Influence des effets d'hystérésis sur les phénomènes de transferts couplés de chaleur et masse en milieux poreux, Thèse de doctorat de l'I.N.P.T., Toulouse (1991).
7. H. Nguyen-Tan, Ecoulements non permanents dans des massifs de milieux poreux non saturés avec effet d'hystérésis, Thèse doctorat d'etat, I.N.P. Toulouse (1978).
8. Y. Mualem, Extension of the similarity hypothesis used for modeling the soil water characteristics, *Water Resour. Res.* **13,** 773–780 (1977).
9. C. H. A. Molenda, P. Crausse, J. Cid and D. Lemarchand, Etude des phénomènes de transfert de chaleur et d'humidité en béton cellulaire, Rapport GEMP, IMFT, Toulouse (1990).
10. D. Quenard and H. Salle, Contribution à la caractérisation hygrothermique du béton cellulaire autoclavé, Rapport GM/88-670, CSTB Grenoble (1988).
11. A. V. Luikov, Application of irreversible thermodynamics methods to investigation of heat and mass transfer, *Int. J. Heat Mass Transfer* **9,** 139–152 (1966).
12. W. Kaminski, Hyperbolic heat conduction equation for materials with a nonhomogeneous inner structure, *J. Heat Transfer* **112,** 555–560 (1990).